

Preliminary Expected Performance Characteristics of an APS Multi-Bend Achromat Lattice

Michael Borland for the APS Upgrade Team
ANL/APS/LS-337

CVS revision 1.28: Tue Oct 1 00:11:54 CDT 2013.

1 Introduction

The Advanced Photon Source is the brightest storage ring synchrotron radiation source in the western hemisphere. It is presently in the midst of an upgrade to deliver even higher performance and powerful new capabilities for scientific research using hard x-ray techniques. Recently, it has become accepted that a new avenue for creating high brightness x-ray beams is opening up, based on technology that enables the use of multi-bend achromat (MBA) magnet lattices in the storage ring.

In July, a report by the Basic Energy Sciences Advisory Committee (BESAC) [1] recommended considering the incorporation of this new technology to enhance research facilities such as the APS. Hence, the APS Upgrade is exploring how the incorporation of an MBA lattice into the on-going project can optimize the scientific capabilities.

To facilitate discussion of the scientific impact and design optimization of such a lattice, this document describes the expected performance characteristics calculated for an initial “straw-man” design. Since the design is still being developed, these characteristics may change in the future as they are optimized with community input.

A primary benefit of the MBA lattice is to dramatically increase x-ray brightness, which is achieved by implementing four improvements, listed here in order of importance:

- Reducing the electron beam emittance from the present value of 3.1 nm (or nm-rad) to under 100 pm.
- Tuning the beta functions at the insertion devices closer to the optimum values of L_u/π , where L_u is the undulator length.
- Deploying optimized small-gap insertion devices.
- Increasing the beam current to 200 mA.

Additional design goals include enhancing the x-ray flux and the per-pulse brightness and flux, which are further characteristics that benefit the scientific capabilities.

1.1 Electron Beam Properties

The zero-current natural emittance in an electron storage ring is governed by [2, 3]

$$\epsilon_0 \sim C_\epsilon \frac{E^2}{N_s^3 N_d^3}, \quad (1)$$

where C_ϵ is a constant, E is the beam energy, N_s is the number of sectors (40 in the case of APS), and N_d is the number of dipole (or bending) magnets per sector. The present APS lattice runs at $E = 7$ GeV and has $N_d = 2$. The MBA lattice design described here has $N_d = 7$, which implies an approximately 40-fold reduction the natural emittance. In this initial design, we have chosen a beam energy of 6 GeV, which appears necessary to make the magnet strengths tractable. However, the choice of beam energy is a complex matter and has yet to be fully explored.

Typically, we expect that $\epsilon_0 = \epsilon_x + \epsilon_y$, where ϵ_x and ϵ_y are the emittances in the horizontal and vertical planes, respectively. This is often parametrized by the emittance ratio κ

$$\begin{aligned} \epsilon_y &= \frac{\kappa}{1+\kappa} \epsilon_0 \\ \epsilon_x &= \frac{1}{1+\kappa} \epsilon_0 \end{aligned} \quad (2)$$

These equations are strictly correct only in the limit of zero current. For non-zero current, particularly when the natural emittance or κ are very small, the emittance and energy spread of the bunch may increase as a result of intra-beam scattering. This effect is more severe when the current in a bunch is higher and when the bunch is short. Increasing κ and stretching the bunch are effective methods of reducing the impact of intra-beam scattering.

1.2 X-ray Brightness

With some simplifying assumptions, the x-ray brightness B of an undulator source in an electron storage ring is governed by

$$B = \frac{F_s}{4\pi^2 \Sigma_x \Sigma_{x'} \Sigma_y \Sigma_{y'}}, \quad (3)$$

where F_s is the spectral flux (typically stated in units of photons/second/0.1%BW), $\Sigma_{x,y}$ are the total rms photon beam sizes for the horizontal and vertical planes, and $\Sigma_{x',y'}$ are the total rms divergences. The total rms beam sizes are obtained by convolving the electron beam distribution with the radiation distribution emitted by a single electron traversing an undulator. Assuming uncorrelated gaussian beams, these convolutions give

$$\Sigma_q = \sqrt{\epsilon_q \beta_q + \epsilon_r \beta_r}, \quad (4)$$

for the sizes, while the divergences are

$$\Sigma_{q'} = \sqrt{\frac{\epsilon_q}{\beta_q} + \frac{\epsilon_r}{\beta_r}}, \quad (5)$$

where q is x or y , ϵ_q is the electron beam emittance, and β_q is the electron beam beta function. The quantities ϵ_r and β_r are the emittance and beta function of the monochromatized undulator radiation emitted by a single electron. For photons of wavelength λ from an undulator of length L_u , these are roughly given by

$$\epsilon_r = \frac{\lambda}{2\pi} \quad (6)$$

and

$$\beta_r = \frac{L_u}{\pi}, \quad (7)$$

giving

$$\sigma_{r'} = \sqrt{\frac{\epsilon_r}{\beta_r}} = \sqrt{\frac{\lambda}{2L_u}} \quad (8)$$

and

$$\sigma_r = \sqrt{\epsilon_r \beta_r} = \frac{1}{2\pi} \sqrt{2\lambda L_u}. \quad (9)$$

(Note that these values assume detuning of the undulator to maximize flux [4] and are in any case only approximate.)

To maximize brightness, we must minimize the denominator of Equation (3). This entails minimizing the products $\Sigma_x \Sigma_{x'}$ and $\Sigma_y \Sigma_{y'}$. While ϵ_q should ideally be small compared to ϵ_r , this is not always possible, particularly for short wavelengths. In practical units,

$$\epsilon_r [\text{pm}] \approx \frac{200}{E_p [\text{keV}]} \approx 16 \lambda_p [\text{\AA}] \quad (10)$$

For example, for 10 keV, we have $\epsilon_r = 20$ pm. The virtue of the MBA lattice is that we can approach this value much more closely than is possible with the present lattice. Note that when ϵ_r and ϵ_q are comparable, it is important to have $\beta_q \approx \beta_r$.

2 Global Accelerator Properties

Some global properties of the accelerator design described here are listed in Table 1. The circumference and number of sectors are, of course, unchanged from the present machine, although in fact the circumference would change slightly to accommodate the change in geometry that results from having bending in different locations. Although there are many more dipoles in a sector, we anticipate only a single bending magnet beamline in each sector, as in the present machine. The average pressure is expected to be quite low in spite of the narrow vacuum pipe, owing to the use of NEG-coated chambers. This should ensure similar bremsstrahlung radiation levels as seen at present.

Quantity	Symbol	Range	Units
Circumference	C	1104	m
Number of sectors	N_s	40	
Number of dipoles per sector	N_d	5-8	
Arc beam pipe outside diameter	D_p	26	mm
Average pressure	P_{ave}	< 2	nT

Table 1: Global accelerator properties

3 Basic Electron Beam Properties

The basic properties of the electron beam in this design are listed in Table 2. The major changes from the present-day APS are the dramatic drop in horizontal and vertical emittance, as well as a decrease in the beam energy from 7 to 6 GeV. The expected fractional rms energy spread would be very similar to the present value.

The natural emittance is expected to be in the range of 60 to 80 pm, which would be closely realized only for fill patterns with small single-bunch charge. Due to intra-beam scattering (IBS), the emittance would grow somewhat for fill patterns with few bunches. It is thought that the maximum single-bunch charge would be similar to that of the present APS 24-bunch mode (~ 15 nC or 4.2 mA per bunch). Typically in cases with higher single bunch charge we would increase κ to reduce the impact on beam lifetime.

Quantity	Symbol	Range	Units
Beam energy	E	6	GeV
Natural emittance	ϵ_0	60 - 80	pm
Rms energy spread	σ_δ	0.09 - 0.12	%
Emittance ratio	$\kappa = \epsilon_y/\epsilon_x$	0.1 - 1.0	
Emittance increase due to IBS	-	< 25	%
Horizontal emittance	ϵ_x	30 - 91	pm
Vertical emittance	ϵ_y	40 - 5	pm

Table 2: Basic electron beam properties

4 Fill Pattern

Table 3 shows the timing parameters for simple fill patterns consisting of uniformly spaced single bunches, using a maximum current per bunch of 4.2 mA (15 nC bunch charge). For uniformly spaced single bunches, the 48 bunches needed for 200 mA would have a spacing of 77 ns. Many other fill patterns are possible, such as uniformly spaced multiplets, with larger times between multiplets (and 2.8 ns between bunches within a multiplet), or hybrid fills with part of the ring filled with widely spaced singlets and the remainder of the bunches grouped more closely. Note that improved opening speeds for choppers to separate bunches for timing applications should be possible because of the smaller beam sizes.

As noted above, because of intra-beam scattering these few-bunch patterns will have increased coupling compared to many-bunch fills. Table 7 shows more detailed parameters.

Quantity	Symbol	Range	Units
Total current	I	200	mA
Number of bunches	N_b	48-324	
Bunch rate	f_b	13-88	MHz
Rms bunch duration	σ_t	70-18	ps

Table 3: Parameters of simple uniform fill patterns

5 Insertion Device Sources

Ranges of insertion device source points of this design have the properties listed in Table 4. These values are stated for the centers of the straight sections. Devices offset from this position would see somewhat different parameters. Although ranges of values are given, this should not be interpreted as indicating that individual straight sections would have different values from others. The intention is to deliver the same values at all straight sections, in order to maintain the symmetry of the lattice. Detailed properties for the latest revision are given in Section 7.

Quantity	Symbol	MBA Range	Present-day	Units
Horizontal beta function	β_x	1-4	19.5	m
Horizontal dispersion function	η_x	< 3	170	mm
Horizontal beam size	σ_x	5 - 19	275	μm
Horizontal beam divergence	$\sigma_{x'}$	3 - 10	11	μrad
Horizontal size-divergence product	$\sigma_x \sigma_{x'}$	30 - 91	3100	pm
Vertical beta function	β_y	1-4	2.9	m
Vertical dispersion function	η_y	0	0	mm
Vertical beam size	σ_y	2 - 13	10	μm
Vertical beam divergence	$\sigma_{y'}$	1 - 6	3.5	μrad
Vertical size-divergence product	$\sigma_y \sigma_{y'}$	5 - 40	35	pm

Table 4: Insertion device source point characteristics

Insertion device straight sections would accommodate insertion devices with properties listed in Table 5. Note that the maximum *magnetic* length for superconducting undulators (SCUs) would be

significantly shorter than the value listed; a magnetic length of 3.7 m is a reasonable assumption for SCUs.

Quantity	Symbol	Range	Units
Maximum length	L_u	4.8	m
Vertical chamber inside gap	g_v	≥ 6	mm
Horizontal chamber inside gap	g_h	≥ 6	mm
Vertical magnet gap	m_v	≥ 8.5	mm
Horizontal magnet gap	m_h	≥ 8.5	mm

Table 5: Insertion device properties

Figures 1 through 4 show calculations of the x-ray brightness and flux (both average and per pulse) anticipated from this MBA lattice design, compared with those for the present-day APS. All insertion devices were assumed to be the maximum possible length of 4.8 m for permanent-magnet devices and 3.7 m for SCUs. The devices were chosen to represent the potential improvements, rather than exhaustively catalog the possibilities. Other choices of undulator period should provide similar improvements of two or more orders of magnitude in brightness at hard x-ray energies above a few keV. For the present APS, we used 100 mA beam current with 4.8-m-long 33-mm-period and 27-mm-period devices with 10.75-mm magnetic gaps. For the MBA lattice, we used 4.8-m-long 25 and 28-mm period permanent magnet devices and 3.7-m-long 15.5- and 20.5-mm period devices, all with 8.5-mm magnetic gaps. In all cases, we assumed 200 mA stored current in the MBA lattice with $\epsilon_0 = 80$ pm. For the average brightness computation, we assumed $\kappa = 0.1$, while for the pulse brightness and flux we assumed $\kappa = 1$, since this will be needed to minimize IBS effects. All calculations assume the use of the existing APS high-heat-load front-end design [5].

Unlike the present-day APS ring, we expect that an MBA lattice would be operated in on-axis injection mode (“swap-out” instead of “top-up”) [6, 7]. Because of this, we should not be restricted to traditional insertion devices with small vertical gaps and relatively large horizontal gaps. Instead, we should be able to use devices with small horizontal gaps as well, opening the possibility of vertical and helical undulators. For example, superconducting helical devices producing circular polarization may be workable for the first time in a lightsource storage ring. (Note that impedance considerations will limit the number of devices with small gaps in both planes.)

Despite the higher current and dramatically higher brightness of this design, the total power and power density from optimized undulators would be less than or comparable to the power and power density from existing APS undulators. This may be understood by noting that the angular spread of the white beam from an undulator is K/γ , with no dependence on the beam emittance [8].

6 Bending Magnet Sources

Because of the decreased electron beam energy, a high-field insertion must be used to increase the critical energy of bending magnet radiation. Details are yet to be determined. Goals for bending magnet source properties are listed in Table 6.

Quantity	Symbol	Range	Units
Critical energy	E_c	15-20	keV
Radiation fan width	θ_B	> 5	mrad

Table 6: Goals for bending magnet source properties

7 Details for Latest Lattice Revision

Table 7 shows detailed ID source point properties as a function of the number of bunches N_b . Listed are the emittance ratio κ , the rms horizontal and vertical emittances $\epsilon_{x,y}$, the rms horizontal and vertical beamsizes $\sigma_{x,y}$, the rms horizontal and vertical divergences $\sigma'_{x,y}$, the rms bunch duration σ_t , the rms energy spread σ_δ , the 10th-percentile predicted Touschek lifetime $\tau_{10^{th}}$, and the approximate injection interval ΔT_{inj} . In most cases, several bunch durations are listed, including a minimum duration plus durations of approximately 35 and 70 ps. κ is adjusted to attempt to maintain the 10th-percentile predicted lifetime $\tau_{10^{th}}$ above 3 hours.

Table 7: Parameters for ID source points for H7BA-TwoSector-60pm-nux105-nuy34

κ	σ_t ps	ϵ_x pm	ϵ_y pm	β_x m	β_y m	σ_x μm	σ'_x μrad	σ_y μm	σ'_y μrad	σ_δ 10^{-4}	$\tau_{10^{th}}$ hour	ΔT_{inj} s
				$N_b = 48$		$f_b = 13.0\text{MHz}$						
1.00	70	41.7	41.7	1.3	2.9	7.4	5.7	10.9	3.8	9.95	1.38	10.4
				$N_b = 81$		$f_b = 22.0\text{MHz}$						
1.00	35	42.5	42.5	1.3	2.9	7.4	5.7	11.0	3.9	1.00×10^1	1.19	5.3
1.00	69	39.6	39.6	1.3	2.9	7.2	5.5	10.6	3.7	9.77	2.23	9.9
				$N_b = 162$		$f_b = 44.0\text{MHz}$						
1.00	21	41.6	41.6	1.3	2.9	7.3	5.7	10.9	3.8	9.95	1.41	3.1
1.00	35	39.6	39.6	1.3	2.9	7.2	5.5	10.6	3.7	9.77	2.23	5.0
0.24	68	56.1	13.3	1.3	2.9	8.5	6.6	6.2	2.2	9.74	3.00	6.7
				$N_b = 216$		$f_b = 58.7\text{MHz}$						
1.00	20	40.7	40.7	1.3	2.9	7.3	5.6	10.8	3.8	9.86	1.72	2.9
1.00	34	38.8	38.8	1.3	2.9	7.1	5.5	10.5	3.7	9.70	2.91	4.9
0.11	68	61.4	6.5	1.3	2.9	8.9	6.9	4.3	1.5	9.79	3.00	5.0
				$N_b = 324$		$f_b = 88.0\text{MHz}$						
1.00	18	39.5	39.5	1.3	2.9	7.2	5.5	10.6	3.7	9.76	2.32	2.6
0.22	35	56.6	12.6	1.3	2.9	8.6	6.6	6.0	2.1	9.74	3.00	3.3
0.10	68	59.8	5.9	1.3	2.9	8.8	6.8	4.1	1.4	9.69	4.31	4.8

References

- [1] Report of the BESAC Subcommittee on Future X-ray Light Sources, July 2013. science.energy.gov/media/bes/besac/pdf/Reports/Future_Light_Sources_report_BESAC_approved_72513.pdf.
- [2] J. Murphy. Synchrotron light source data book. Technical Report BNL-42333, BNL, January 1989.
- [3] H. Wiedemann. *Particle Accelerator Physics II*. Springer, Berlin, 1999.
- [4] P. Elleaume. *Undulator radiation*, page 69. Taylor and Francis, London, 2003.
- [5] Y. Jaski. New front-end design for multiple in-line undulators at the advanced photon source. In *Proc. of SRI 2004*, volume 705, pages 356 – 359. AIP Conf. Proc., 2004.

- [6] M. Borland. Can APS Compete with the Next Generation?, May 2002. Presented at APS Strategic Planning Workshop.
- [7] L. Emery and M. Borland. Possible Long-Term Improvements to the Advanced Photon Source. In *Proc. of PAC 2003*, pages 256–258, 2003.
- [8] Kwang-Je Kim. Angular distribution of undulator power for an arbitrary deflection parameter K . *NIM A*, pages 67–70, 1986.

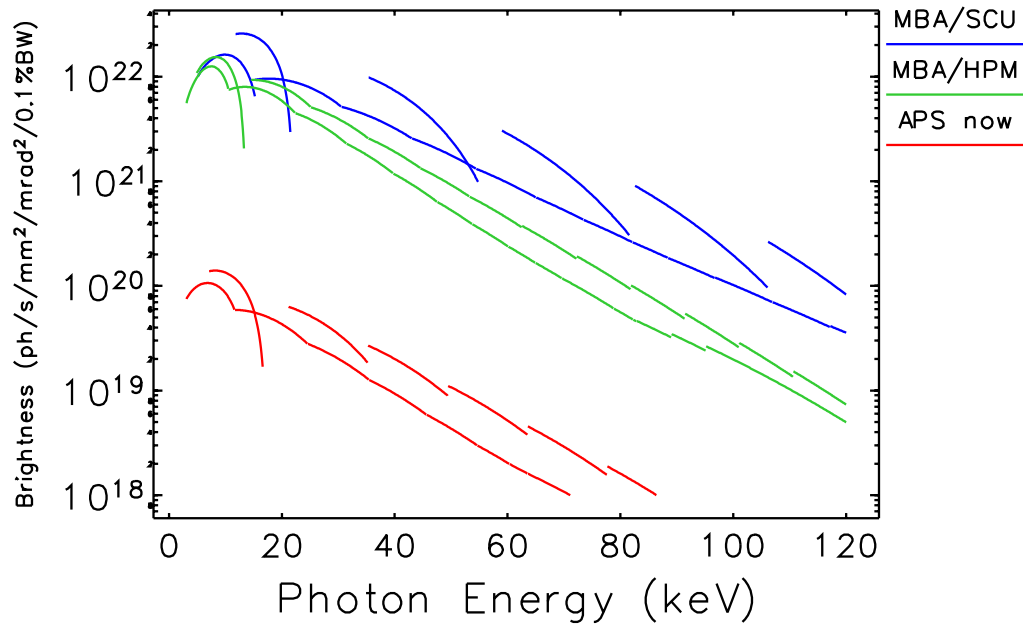


Figure 1: Comparison of brightness from the present APS to selected hybrid-permanent magnet and superconducting undulators in the MBA lattice design described here. See text for details.

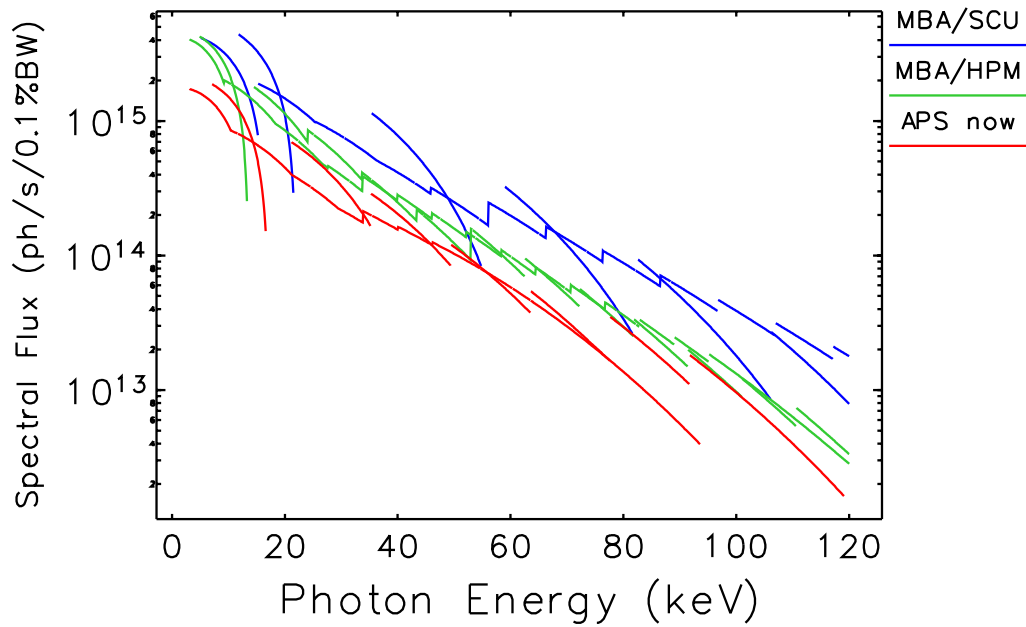


Figure 2: Comparison of flux from the present APS to selected hybrid-permanent magnet and superconducting undulators in the MBA lattice design described here. See text for details.

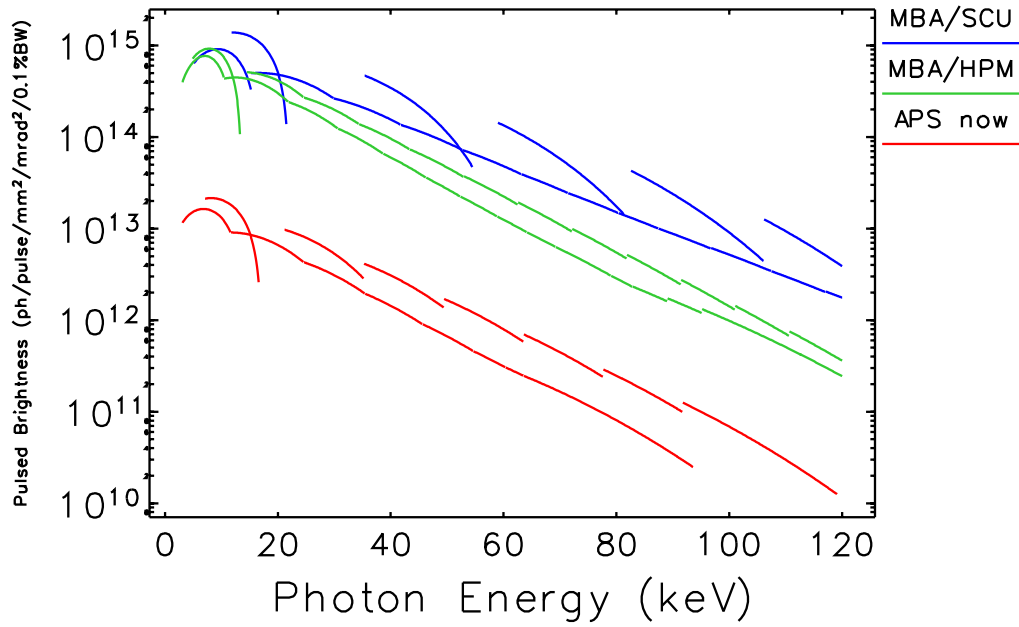


Figure 3: Comparison of pulsed brightness from the present APS to selected hybrid-permanent magnet and superconducting undulators in the MBA lattice design described here. See text for details.

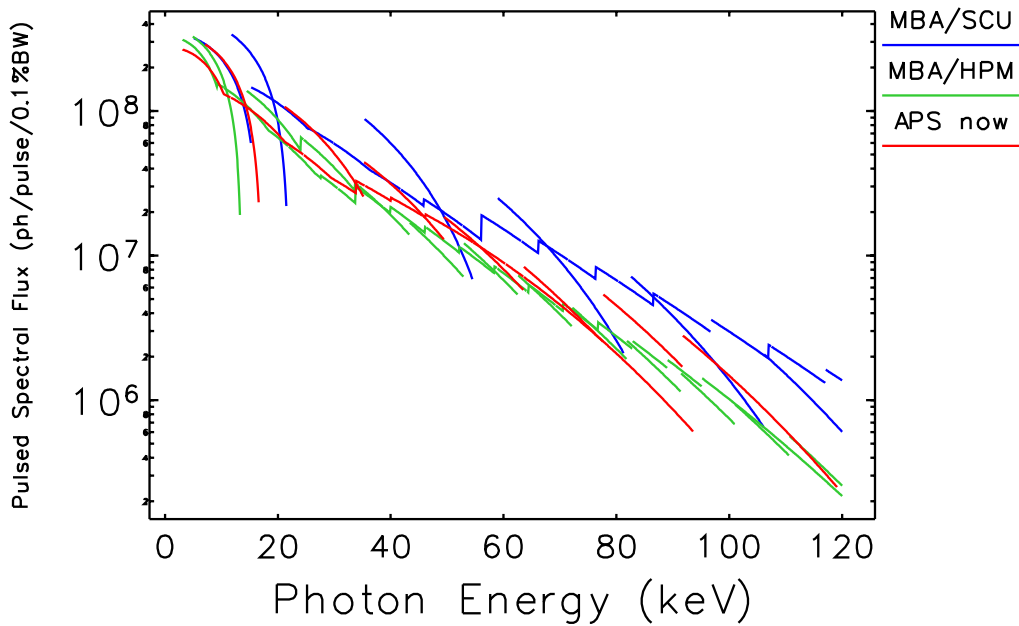


Figure 4: Comparison of pulsed flux from the present APS to selected hybrid-permanent magnet and superconducting undulators in the MBA lattice design described here. See text for details.